



Short communication

## An imidazolium based ionic liquid electrolyte for lithium batteries

Jae-Kwang Kim<sup>a,\*</sup>, Aleksandar Matic<sup>a</sup>, Jou-Hyeon Ahn<sup>b</sup>, Per Jacobsson<sup>a</sup>

<sup>a</sup> Department of Applied Physics, Chalmers University of Technology, 412 96 Göteborg, Sweden

<sup>b</sup> Department of Chemical & Biological Engineering and Engineering Research Institute, Gyeongsang National University, 900, Gajwa-dong, Jinju 660-701, Republic of Korea

### ARTICLE INFO

#### Article history:

Received 11 December 2009

Received in revised form 2 June 2010

Accepted 2 June 2010

Available online 10 June 2010

#### Keywords:

Ionic liquid electrolyte

PMIMTFSI

Ion–ion interaction

Ionic conductivity

Lithium batteries

### ABSTRACT

An electrolyte for lithium batteries based on the ionic liquid 3-methyl-1-propylimidazolium bis(trifluoromethylsulfonyl)imide (PMIMTFSI) complexed with lithium bis(trifluoromethylsulfonyl)imide (LiTFSI) at a molar ratio of 1:1 has been investigated. The electrolyte shows a high ionic conductivity ( $\sim 1.2 \times 10^{-3} \text{ S cm}^{-1}$ ) at room temperature. Over the whole investigated temperature range the ionic conductivity is more than one order of magnitude higher than for an analogue electrolyte based on N-butyl-N-methyl-pyrrolidinium bis(trifluoromethanesulfonyl)imide (Py<sub>14</sub>TFSI) complexed with LiTFSI and used here as a benchmark. Raman results indicate furthermore that the degree of lithium coordinated TFSI is slightly lower in the electrolyte based on PMIMTFSI and thus that the Li<sup>+</sup> charge carriers should be higher than in electrolytes based on Py<sub>14</sub>TFSI. An ionic liquid gel electrolyte membrane was obtained by soaking a fibrous fully interconnected membrane, made of electrospun P(VdF–HFP), in the electrolyte. The gel electrolyte was cycled in Li/ionic liquid polymer electrolyte/Li cells over 15 days and in Li/LiFePO<sub>4</sub> cells demonstrating good interfacial stability and highly stable discharge capacities with a retention of >96% after 50 cycles ( $\sim 146 \text{ mAh g}^{-1}$ ).

Crown Copyright © 2010 Published by Elsevier B.V. All rights reserved.

### 1. Introduction

The search for highly stable electrolytes for lithium batteries has been intense in recent years, especially for larger batteries suitable for transportation applications such as in electric vehicles (EVs) and hybrid-electric vehicles (HEVs). Since the first report of room temperature ionic liquids (RTILs) based on 1-ethyl-3-methylimidazolium cation and tetrafluoroborate anion by Wilkes and Zaworotko [1], a number of RTILs have gained considerable attention as potential substitutes for the presently used conventional carbonate based solvents for lithium conducting electrolytes. In contrast to electrolytes based on conventional solvents, RTILs, in general, have negligible vapor pressure, non-flammable nature and high thermal stability. In addition the RTILs have intrinsic ionic conductivity at room temperature and a wide electrochemical window, exhibiting good electrochemical stability in the range of 4.0–5.7 V [2,3]. However, one important disadvantage to the application of RTILs in electrolytes is a relatively high viscosity compared to conventional liquid electrolytes; the high viscosity limits ionic mobility and therefore also ionic conductivity.

RTILs are molten salts composed of only cations and anions. The cation, for example based on imidazolium, pyrrolidinium, piperidinium, phosphonium and pyridinium, can be modified by incorporation of side groups to the carbon atoms of the

ring. With a large number of possible anions, for example [BF<sub>4</sub>]<sup>−</sup>, [PF<sub>6</sub>]<sup>−</sup>, [N(CN)<sub>2</sub>]<sup>−</sup>, [C<sub>4</sub>F<sub>9</sub>SO<sub>3</sub>]<sup>−</sup>, [CF<sub>3</sub>CO<sub>2</sub>]<sup>−</sup>, [CF<sub>3</sub>SO<sub>3</sub>]<sup>−</sup>, [N(CF<sub>3</sub>SO<sub>2</sub>)<sub>2</sub>]<sup>−</sup>, and [CF<sub>3</sub>CONCF<sub>3</sub>SO<sub>2</sub>]<sup>−</sup> the properties of a RTIL can be tailored through the selection of cation and anion [2–10]. Several attempts have been made to tailor new RTILs intended as solvents for lithium salts; some examples are N-alkyl-N-methylmorpholinium bis(trifluoromethylsulfonyl)imide, triethyl (methoxymethyl)phosphonium bis(trifluoromethylsulfonyl)amide and trialkylsulfonium dicyanamides [11–13]. However, so far the ionic conductivity obtained has been smaller than what could be expected based on the viscosity and the concentration of ionic charge carriers in these systems. Thus indicating a high degree of ion–ion interaction; resulting for example in clusters of Li coordinated TFSI or ion pairing [10,14]. Furthermore the systems mentioned above show low electrochemical stability compared to more common RTILs [2]. Recently, also RTILs of the electrochemically more stable pyrrolidinium cation group has been studied for application towards lithium batteries [15–19]. These pyrrolidinium based systems show promising results although they have the drawback of being rather poor solvents for lithium salts which in turn limits the number of effective charge carriers and furthermore results in a rapid increase of viscosity with increasing lithium salt concentration and with decreasing temperature. Nevertheless, electrolytes based on N-butyl-N-methyl-pyrrolidinium bis(trifluoromethanesulfonyl)imide (Py<sub>14</sub>TFSI) complexed with a lithium salt can be considered as a good benchmark for ionic liquid-based electrolytes. An important issue when applying RTILs in electrolytes is the ability to form a solid electrolyte interface (SEI).

\* Corresponding author.

E-mail address: [jaekwang@chalmers.se](mailto:jaekwang@chalmers.se) (J.-K. Kim).

The SEI have seemingly contradictory properties; it prevents undesirable reactions between the ionic liquid electrolyte (ILE) and the electrode at the cost of increased resistance and decreased capacity due to consumption of lithium. However, the latter can possibly be solved by addition of additives to the electrolyte or by a substitution of electrode material [20–22].

In the present publication we present an electrochemical and spectroscopic study of an ionic liquid electrolyte based on 1-propyl-3-methylimidazolium bis(trifluoromethylsulfonyl)imide (PMIMTFSI) and complexed with LiTFSI to a molar ratio of 1:1. For comparison results on a Py<sub>14</sub>TFSI based analogue electrolyte are presented. The PMIMTFSI based electrolyte LiTFSI is used here as electrolyte in a gel type lithium secondary battery. Our results demonstrate a good stability and highly stable discharge capacity of the battery based on this electrolyte.

## 2. Experimental

### 2.1. Preparation of ionic liquid-based gel polymer electrolyte and cathode

The ionic liquids, PMIMTFSI and Py<sub>14</sub>TFSI together with the LiTFSI were all obtained from Aldrich ( $\geq 98\%$  purity), stored under argon and used as received. Fibrous P(VdF-HFP) membranes were prepared by electrospinning according to the method described previously [23,24]. A 16 wt.% solution of P(VdF-HFP) (Kynar Flex 2801) in a mixed solvent of acetone and N,N-dimethylacetamide (HPLC grades, Aldrich) in 7:3 wt. ratio was electrospun at room temperature. A homogenous, free standing film of  $\sim 80 \mu\text{m}$  thickness was obtained. The membrane has a porous structure of entwined polymer fibers of  $\sim 1 \mu\text{m}$  average thickness forming a net with a mesh size of  $\sim 5 \mu\text{m}$  [23]. An ionic liquid gel polymer electrolyte (ILPE) was obtained by soaking the polymer membrane for 30 s in a solution of LiTFSI/PMIMTFSI (1:1 molar ratio) under argon atmosphere at room temperature. The ILPE obtained is transparent and mechanically stable with good retention of the electrolyte, the latter a requirement for application in lithium batteries [23,24]. The LiFePO<sub>4</sub> cathode material was prepared by mechanical activation method as described in detail elsewhere [25,26].

### 2.2. Characterization techniques

The ionic conductivity of the pure ionic liquids and the lithium salt containing ionic liquids were measured from  $-20$  to  $80^\circ\text{C}$  in a gold-plated cell with a 1 mm Teflon spacer, over a frequency range  $10^{-1}$  to  $10^6$  Hz using a Novocontrol broadband dielectric spectrometer.

Raman spectra of the ionic liquids and the ionic liquid electrolytes were recorded on a Bruker IFS 66 Fourier Transform spectrometer, equipped with a FRA 106 Raman module and using the 1064 nm line of a Nd:YAG laser as excitation source. The laser power was set to 250 mW and the resolution was  $4 \text{ cm}^{-1}$ .

For the electrochemical measurements the LiFePO<sub>4</sub> active material powder, carbon black and poly(vinylidene fluoride) (PVdF: Aldrich) binder were mixed in the ratio 83:7:10 by weight in N-methyl pyrrolidone (NMP) solvent and the viscous slurry was cast on aluminum foil and dried at  $95^\circ\text{C}$  under vacuum for 12 h. The film was cut into circular discs of area  $0.95 \text{ cm}^2$  and mass  $\sim 3.0 \text{ mg}$  for use as the cathode. Cyclic voltammetry (CV) measurements of a Li/ILPE/Li cell were performed at  $25^\circ\text{C}$  at a scan rate of  $1 \text{ mV s}^{-1}$  between  $-1$  and  $+1 \text{ V}$ . The interfacial resistance between the ILPE and the lithium metal electrode was measured by analyzing the impedance response over the frequency range of  $10^{-2}$  to  $10^6$  Hz of the Li/ILPE/Li cell kept at room temperature for a period of up to 15 days. Electrochemical performance tests were carried out using an

automatic galvanostatic charge–discharge unit, WBCS3000 battery cyler, between 2.5 and 4.0 V. The experiments were performed at  $0.1 \text{ C}$  ( $0.042 \text{ mA cm}^{-2}$ ) current density rate.

## 3. Results and discussion

The temperature dependence of the ionic conductivity of pure ILs and the ILs complexed with LiTFSI is shown in Fig. 1. The conductivity of all four systems increases with increasing temperature over the investigated temperature range. The measured conductivity for the pure PMIMTFSI and the PMIMTFSI/LiTFSI electrolyte is in excellent agreement with the recently published results by Guerfi et al. [27] while the measured conductivity for pure Py<sub>14</sub>TFSI is slightly higher (about 20%) than the results reported in Ref. [18]. As is generally observed the overall conductivity of an IL decreases with complexation of a salt. However, over the whole temperature range investigated this decrease is more pronounced for the Py<sub>14</sub>TFSI based system. As a result the conductivity of the PMIMTFSI/LiTFSI electrolyte is about an order of magnitude higher compared to the Py<sub>14</sub>TFSI based analogue over temperature. Arguably a reasonable high ion conductivity ( $>10^{-4} \text{ S cm}^{-1}$ ) is needed for high power battery applications [28]; a conductivity of around  $1.2 \times 10^{-4} \text{ S cm}^{-1}$  is achieved at  $0^\circ\text{C}$  in the PMIMTFSI based system increasing to around  $1.2 \times 10^{-3} \text{ S cm}^{-1}$  at  $30^\circ\text{C}$ . Before passing it is to be noted that the conductivity of the gel polymer electrolyte is not reported in the present study. A decrease in the conductivity can be anticipated in part due to the dilution of charge carrier concentration per volume caused by the introduction of the P(VdF-HFP) membrane and in part by a nonlinear decrease of diffusion rate of the solvent in a gel as a function of polymer concentration [29]. In PVdF based gel electrolytes with dimethyl ethers a reduction of the total conductivity with a factor of three as compared to the dimethyl ether/Li-salt system has been reported by Abraham et al. [30].

Raman spectra of pure PMIMTFSI and Py<sub>14</sub>TFSI and the electrolyte solutions containing 0.5 M LiTFSI were measured over the frequency range  $0$ – $3500 \text{ cm}^{-1}$ . Raman results of the pure ionic liquids are reported in Fig. 2. The two spectra have several similarities due to the common TFSI anion with main features indicated in the figure. A full assignment of the vibrational modes of the TFSI anion is given in the paper by Duluard et al. [31]. Also some of the vibrational features of the two different cations show similarities, especially and not surprising, in the CH vibrational region  $\sim 2800$ – $3100 \text{ cm}^{-1}$ . It has been established that the strong Raman mode around  $740 \text{ cm}^{-1}$  (shown in the inset of Fig. 2), correspond-

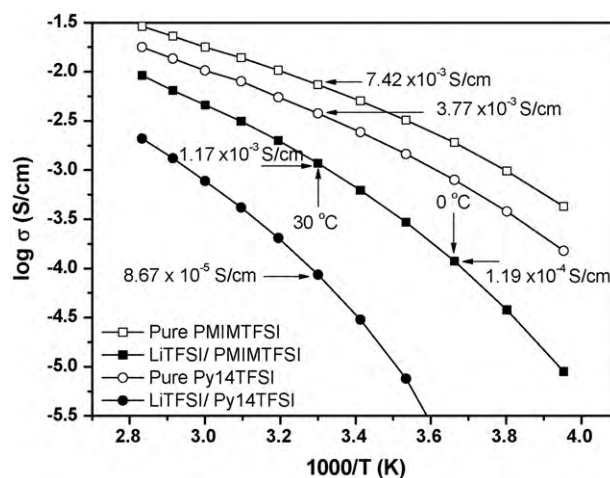
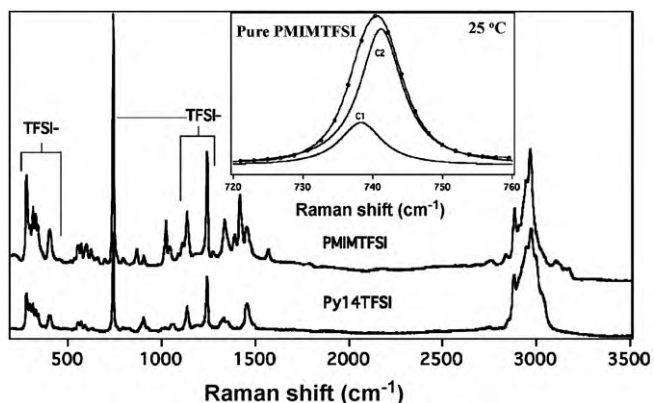


Fig. 1. Ionic conductivity as a function of temperature for pure PMIMTFSI, Py<sub>14</sub>TFSI and the two corresponding liquid electrolytes obtained after complexation with LiTFSI at molar ratio of 1:1.



**Fig. 2.** Raman spectra of PMIMTFSI and Py<sub>14</sub>TFSI at room temperature. Inset: A close up of the strong Raman mode of PMIMTFSI at 740 cm<sup>-1</sup> corresponding to an expansion and contraction mode of the whole TFSI anion that produces a large polarizability change. The contribution of the two conformers (C1 and C2) discussed in text is indicated.

ing to an expansion and contraction mode of the whole TFSI anion that produces a large polarizability change, is sensitive to Li<sup>+</sup> coordinated TFSI and also to the conformational states of the anion [31,32]. In equilibrium the TFSI anion is found in two conformational states, C1 (cisoid) and C2 (transoid) with contributions to the Raman spectra at ~741 cm<sup>-1</sup> at ~745 cm<sup>-1</sup> respectively. The solid lines in the insets are results of a bandfit using Lorentzian profiles.

In Fig. 3(a)–(c) the 740 cm<sup>-1</sup> band for the LiTFSI/PMIMTFSI electrolyte is shown at three different temperatures (-10, 25 and 60 °C). Three conformers are needed to describe the band profile. In addition to the two components related to free C1 and C2 conformers a third component around 748 cm<sup>-1</sup> is found, corresponding to TFSI coordinated to Li ions [31]. With increasing temperature the concentration of TFSI coordinated to Li ions decreases markedly as

observed by the decrease in relative intensity area of the 748 cm<sup>-1</sup> conformer. The concentration of C1 conformer increases while the concentration of C2 conformer is nearly constant over the temperature range. In panel 3(d) the 740 cm<sup>-1</sup> band for the LiTFSI/Py<sub>14</sub>TFSI electrolyte at 25 °C is shown for comparison. When comparing the intensity of the third component in panel (d) with the same component in panel (b) we find that the concentration of TFSI coordinated to Li<sup>+</sup> is ~15% higher than in the corresponding PMIMTFSI based system. We note before passing that the latter result indicates that the major part of the difference in conductivity is related to mobility of the charge carriers.

The compatibility of the ionic liquid-based gel polymer electrolyte, ILPE, vs. a lithium metal electrode has been analyzed by monitoring the complex impedance of a symmetrical Li/ILPE/Li cell over storage up to 15 days at room temperature (see Fig. 4). The symmetrical cell shows a typical impedance resistance pattern for an electrolyte with a high ionic conductivity. The main contribution to the resistance is from the interface while the bulk resistance (the high frequency loci of the arc on the left hand side) is very low. During the first week of storage the total resistance increases (see table inset in Fig. 4). However, during the second week of storage the trend is reversed; the resistance values decreases and stabilizes at an intermediate value. A similar behavior has previously been observed for some gel polymer electrolytes due to improvement of interfacial properties [24,33,34]. The overall increase in resistance might signal a formation of an SEI, however, at this point neither the mechanism nor the composition of such is established.

Cyclic voltammetry (CV) data of the Li/ILPE/Li cell are presented in Fig. 5. The redox peaks in the initial cycle correspond to an anodic oxidation at +0.48 V and a cathodic reduction at -0.41 V vs. Li<sup>+</sup>/Li. A slight shift of the anodic and cathodic voltages is observed up to the fifth cycle. The cell shows nearly overlapping CV curves after about 5 cycles, indicating the occurrence of highly reversible oxidation and reduction processes with high coulombic efficiency. This result

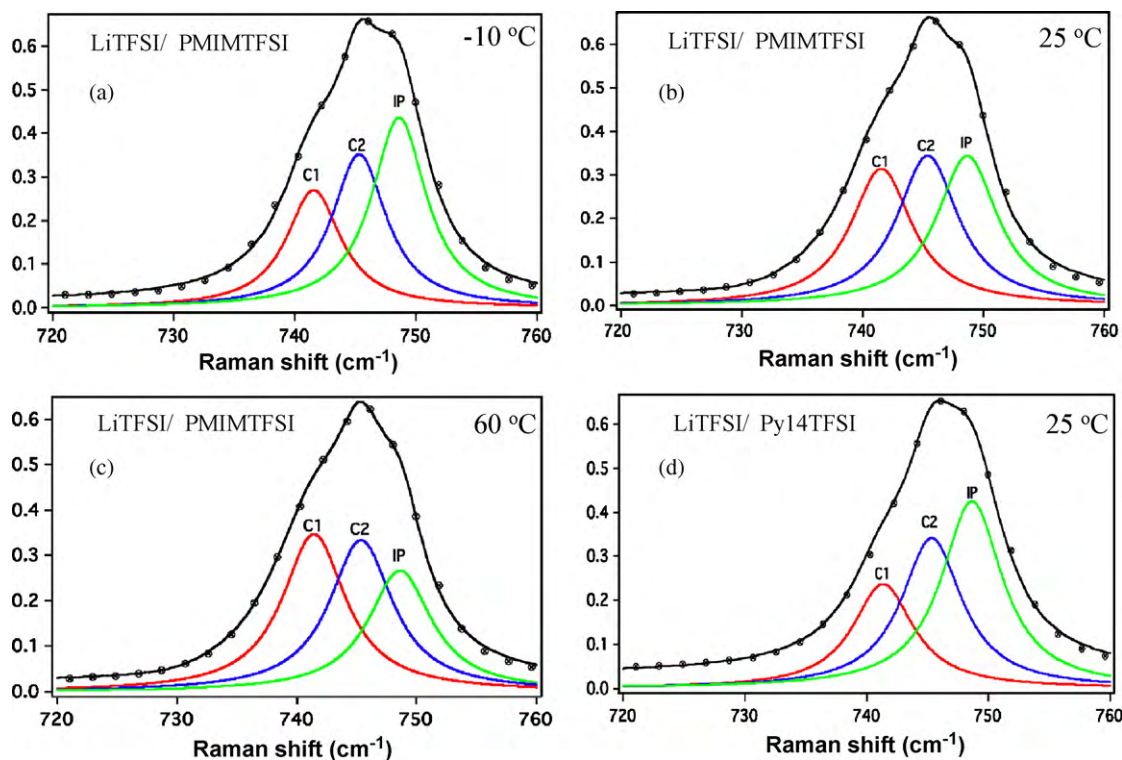


**Fig. 3.** Raman spectra of the 740 cm<sup>-1</sup> mode for different temperatures. Panels (a)–(c) shows the LiTFSI/PMIMTFSI ionic liquid electrolyte at the temperatures indicated and in panel (d) the LiTFSI/Py<sub>14</sub>TFSI electrolyte at 25 °C is shown.

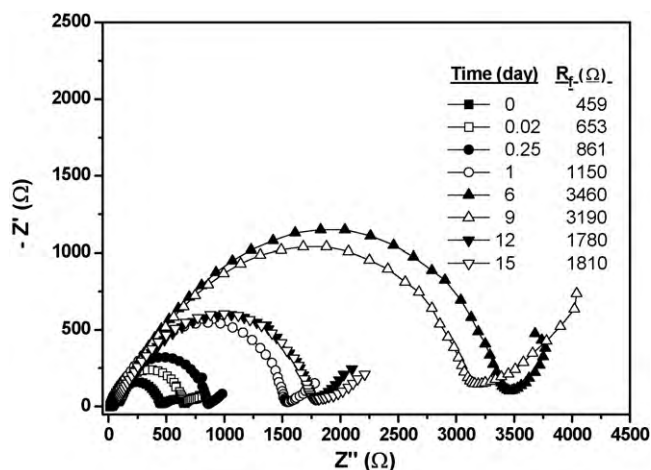


**Fig. 4.** Impedance behavior of the ionic liquid gel polymer electrolyte (ILPE) based on LiTFSI/PMIMTFSI in a Li//ILPE/Li cell as a function of storage time at 25 °C. The total resistance as determined by the low frequency loci of the large semi-circle on the right hand side is tabulated in the inset.

is also in qualitative agreement with the stabilization of the total resistance discussed above.

The charge/discharge behavior at a 0.1C-rate and at room temperature of a Li//ILPE/LiFePO<sub>4</sub> cell during the first 5 cycles is shown in Fig. 6. The charge and discharge capacities are 154.4 and 151.6 mAh g<sup>-1</sup>, respectively, confirming the high coulombic efficiency of the redox process. The initial discharge capacity of the cell corresponds to 89% of the theoretical capacity of LiFePO<sub>4</sub> and is maintained also after 5 cycles. The voltage plateau for the charge and discharge processes is a characteristic of LiFePO<sub>4</sub> [25,26]. The voltage difference between the two plateaus is very small (~0.16 V at first and 0.12 V at fifth cycle) and reflects the low cell resistance that remains stable during cycling. We note that the pronounced plateaus can in part be attributed to a small polarization within the cell at 0.1C-rate. During the first charge discharge cycle the plateaus are however, shorter than in the following cycles. The apparent increase in performance may be attributed to a decrease in internal resistance during the first completed cycle, thereby decreasing the ohmic loss in the battery. The mechanism behind such a decrease is presently unknown to us. Usually, formation of SEI layer on electrode surface involves an irreversible capacity fade. We note, however, that the formation of protective SEI layer in electrolyte

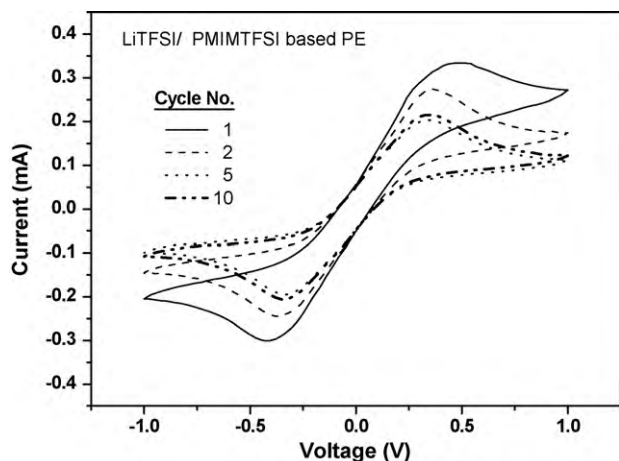


**Fig. 5.** Cyclic voltammetry (CV) curves during 1st, 2nd, 5th and 10th cycles of Li//ILPE/Li cell at 25 °C.

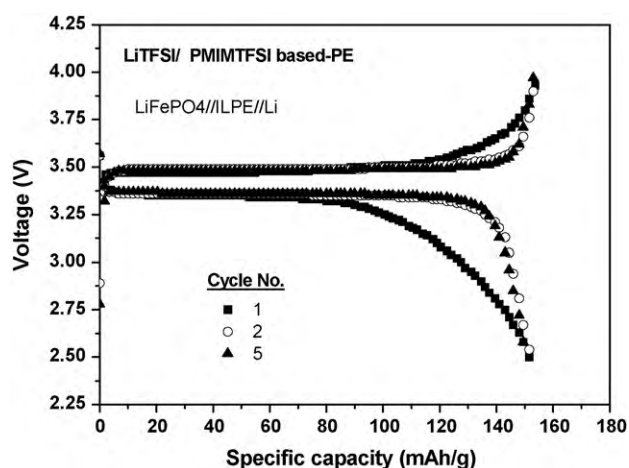


**Fig. 6.** 1st, 2nd and 5th cycles of charge–discharge capacities of a Li/LiFePO<sub>4</sub> cell with the gel polymer electrolyte based on LiTFSI/PMIMTFSI (25 °C, 0.1C-rate, 2.5–4.0 V).

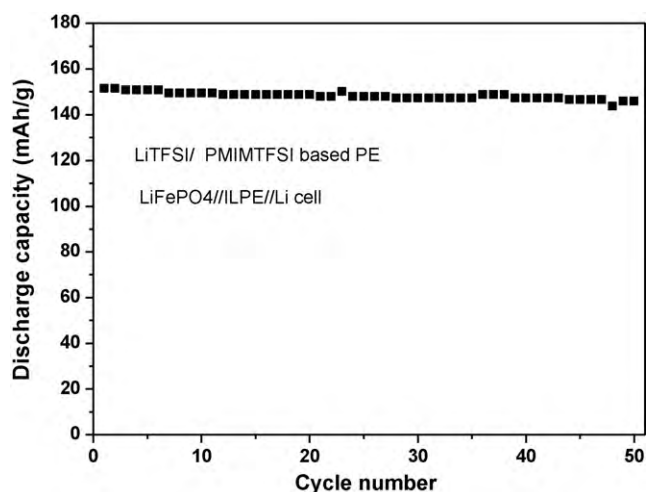


**Fig. 7.** Cycle performance of Li/LiFePO<sub>4</sub> cell with an ionic liquid gel polymer electrolyte based on LiTFSI/PMIMTFSI ionic electrolyte (25 °C, 0.1C-rate, 2.5–4.0 V).

systems based on ionic liquids and lithium salts without further additives have recently been discussed [21].

The discharge capacity as a function of cycle number of a Li//ILPE/LiFePO<sub>4</sub> cell at room temperature under 0.1C-rates is presented in Fig. 7. The cell shows a stable cycling performance over the 50 cycles followed in this work. The discharge capacity fading for the Li//ILPE/LiFePO<sub>4</sub> cell calculated on the basis of the initial and 50th cycle capacities is ~0.08% per cycle. After 50 cycles, a discharge capacity of 145.9 mAh g<sup>-1</sup> was obtained for the cell; thus the capacity retention is 96.2%. The very good cycling performance of the cell is promising and reflects a combination of electrochemical stability of the ionic liquid electrolyte together with excellent conduction properties and compatibility with the electrode materials.

#### 4. Conclusions

The present results demonstrate that LiTFSI/PMIMTFSI in molar ratio 1:1 is a very promising ionic liquid electrolyte for lithium battery application. This is due to a combination of low viscosity, good Li-salt solvation properties and electrochemical stability preventing undesirable reactions between electrode and electrolyte. The LiTFSI/PMIMTFSI electrolyte shows a conductivity above ~10<sup>-4</sup> S cm<sup>-1</sup> at 0 °C, a value proposed as a benchmark for large capacity batteries for EV's or HEV's [28]. Furthermore, it is shown

that the incorporation of the electrolyte in a polymer gel based on electrospun poly(vinylidene fluoride-co-hexafluoropropylene) results in excellent charge/discharge capacity and good cycling stability in a cell with Li/LiFePO<sub>4</sub> electrodes. It is to be noted however, that before the present electrolyte can be suggested for electric vehicle applications thorough testing of long term chemical and thermal stability against for example a graphite anode has to be performed.

### Acknowledgements

The present work was supported by STINT and NRF in a joint Korea-Sweden program.

### References

- [1] J.S. Wilkes, M.J. Zaworotko, *J. Chem. Soc. Chem. Commun.* (1992) 965.
- [2] M. Galiński, A. Lewandowski, I. Stepniak, *Electrochim. Acta* 51 (2006) 5567.
- [3] M. Armand, F. Endres, D.R. MacFarlane, H. Ohno, B. Scrosati, *Nat. Mater.* 8 (2009) 621.
- [4] H.L. Ngo, K. LeCompte, L. Hargens, A.B. McEwen, *Thermochim. Acta* 357/358 (2000) 191.
- [5] M. Holzapfel, C. Jost, P. Novák, *Chem. Commun.* (2004) 2098.
- [6] S. Forsyth, J. Golding, D.R. MacFarlane, M. Forsyth, *Electrochim. Acta* 46 (2001) 1753.
- [7] S. Ferrari, E. Quartarone, P. Mustarelli, A. Magistris, S. Protti, S. Lazzaroni, M. Fagnoni, A. Albini, *Electrochim. Acta* 194 (2009) 45.
- [8] H. Sakaebe, H. Matsumoto, *Electrochem. Commun.* 5 (2003) 594.
- [9] A. Noda, K. Hayamizu, M. Watanabe, *J. Phys. Chem. B* 105 (2001) 4603.
- [10] K.J. Fraser, E.I. Izgorodina, M. Forsyth, J.L. Scott, D.R. MacFarlane, *Chem. Commun.* (2007) 3817.
- [11] K.S. Kim, S. Choi, D. Demberelynamba, H. Lee, J. Oh, B.B. Lee, S.J. Mun, *Chem. Commun.* (2004) 828.
- [12] S. Seki, Y. Umebayashi, S. Tsuzuki, K. Hayamizu, Y. Kobayashi, Y. Ohno, T. Kobayashi, Y. Mita, H. Miyashiro, N. Terada, S.I. Ishiguro, *Chem. Commun.* (2008) 5541.
- [13] D. Gerhard, S.C. Alpaslan, H.J. Gores, M. Uerdingen, P. Wasserscheid, *Chem. Commun.* (2005) 5080.
- [14] J.-C. Lassègues, J. Grondin, C. Aupetit, P. Johansson, *J. Phys. Chem. A* 113 (2009) 305.
- [15] A. Fericola, F. Croce, B. Scrosati, T. Watanabe, H. Ohno, *J. Power Sources* 174 (2007) 342.
- [16] N. Byrne, P.C. Howlett, D.R. MacFarlane, M. Forsyth, *Adv. Mater.* 172 (2005) 2497.
- [17] J.H. Shin, P. Basak, J.B. Kerr, E.J. Cairns, *Electrochim. Acta* 54 (2008) 410.
- [18] G.B. Appetecchi, M. Montanino, D. Zare, M. Carewska, F. Alessandrini, S. Passerini, *Electrochim. Acta* 54 (2009) 1325.
- [19] A. Martinelli, A. Matic, P. Jacobsson, L. Börjesson, A. Fericola, B. Scrosati, *J. Phys. Chem. B* 113 (2009) 11247.
- [20] T. Sato, T. Maruo, S. Marukane, K. Takagi, *J. Power Sources* 138 (2005) 253.
- [21] A. Lewandowski, A. Swiderska-Mocek, *J. Power Sources* 194 (2009) 601.
- [22] J. Hassoun, S. Panero, P. Reale, B. Scrosati, *Adv. Mater.* 21 (2009) 4807.
- [23] X. Li, G. Cheruvally, J.K. Kim, J.W. Choi, J.H. Ahn, K.W. Kim, H.J. Ahn, *J. Power Sources* 167 (2007) 491.
- [24] J.K. Kim, J. Manuel, G.S. Chauhan, J.H. Ahn, H.-S. Ryu, *Electrochim. Acta* 55 (2010) 1366.
- [25] J.K. Kim, J.W. Choi, G. Cheruvally, J.U. Kim, J.H. Ahn, G.B. Cho, K.W. Kim, H.J. Ahn, *Mater. Lett.* 61 (2007) 3822.
- [26] J.K. Kim, G. Cheruvally, J.H. Ahn, G.C. Hwang, J.B. Choi, *J. Phys. Chem. Solids* 69 (2008) 2371.
- [27] A. Guerfi, M. Dontigny, P. Charest, M. Petitclerc, M. Lagacé, A. Vijh, K. Zaghbi, *J. Power Sources* 195 (2010) 845–852.
- [28] J.B. Goodenough, Y. Kim, *Chem. Mater.* 22 (2009) 587.
- [29] T. Uematsu, C. Svanberg, M. Nydén, P. Jacobsson, *Phys. Rev. E* 68 (2003) 051803.
- [30] K.M. Abraham, Z. Jiang, B. Carrol, *Chem. Mater.* 9 (1997) 1978–1988.
- [31] S. Duluard, J. Grondin, J.-L. Bruneel, I. Pianet, A. Grélard, G. Campet, M.-H. Delville, J.-C. Lassègues, *J. Raman Spectrosc.* 39 (2008) 627.
- [32] I. Rey, P. Johansson, J. Lindgren, J.-C. Lassègues, J. Grondin, L. Servant, *J. Phys. Chem. A* 102 (1998) 3249.
- [33] V. Gentili, S. Panero, P. Reale, B. Scrosati, *J. Power Source* 170 (2007) 185.
- [34] C. Gerbaldi, J.R. Nair, G. Meligrana, R. Bongiovanni, S. Bodoardo, N. Penazzi, *Electrochim. Acta* 55 (2010) 1460.